JTTEE5 19:745–755
DOI: 10.1007/s11666-009-9466-3
1059-9630/$19.00 © ASM International

Supervision and Measuring of Particle Parameters During the Wire-Arc Spraying Process with the Diagnostic Systems Accuraspray-g3 and LDA (Laser-Doppler-Anemometry)

S. Zimmermann, E. Vogli, M. Kauffeldt, M. Abdulgader, B. Krebs, B. Rüther, K. Landes, J. Schein, and W. Tillmann

(Submitted July 15, 2009; in revised form September 29, 2009)

Due to low cost of operation, high deposition rates and efficiency, wire arc spraying has become one of the most important thermal spray technologies, especially as a tool for coatings used to improve corrosion and wear protection. In order to obtain high-quality coatings, the flow characteristics of the atomizing gas have to be optimized. Thus, the nozzle design as well as the properties of the gas used need to be adjusted and the resulting particle parameters have to be quantified. Employing the Accuraspray-g3 system in combination with Laser Doppler Anemometry (LDA), the particle size distribution and velocity have been measured for a wide range of parameters, including different materials, different gas pressures and nozzles resulting in design suggestions and offering the possibility to compare the two different diagnostic systems.

Keywords arc spraying, cored wires, diagnostics and control, influence of spray parameters

1. Introduction

Wire-arc spraying technology offers lower operating costs, higher deposition rates and better efficiencies compared to other thermal spraying systems (Ref 1). Wire arc sprayed coatings cover a broad range of applications in the field of wear resistance and corrosion protection. Fields-of-use include off-shore area applications, paper manufacturing and bonding layer production for applying ceramic layers or to metalize plastic substrates. In addition, it is possible to manufacture so-called pseudo-alloys through arc spraying of two or more different feedstock wires (Ref 2).

The quality of wire arc sprayed coatings depends on the particle formation process as well as on the kinetic behavior and the interaction of particles with the surrounding environment during flight. These characteristics are controlled to a large extent by the specific properties of the atomization gas, by wire feedstock parameters as well as by process parameters, such as nozzle shape, atomization gas pressure, voltage, current and stand-off distance. Already small deviations of the optimized spraying parameters can lead to deteriorated mechanical and technological properties of sprayed coatings. An exact knowledge of the in-flight particle behavior and an on-line diagnostics of spraying processes are necessary to assure a high quality and reproducibility of the coatings produced (Ref 3).

Diagnostic methods play a decisive role to evaluate the thermal and kinetic energy of generated particles during the arc spray process. In the last decades different diagnostic methods have been developed and used to study the thermal spraying processes (Ref 4). To measure particle velocity and particle size formed during thermal spraying optical methods, such as Laser-Doppler-Anemometry (LDA) (Ref 5), Particle Image Velocimetry (PIV) (Ref 6), Laser Two Focus (L2F) (Ref 7) or Particle Shape Imaging (PSI) (Ref 8) have been employed, while systems such as Accuraspray-g3, SprayWatch or DPV2000 (Ref 9-11) have been used to define apart from velocity also the particle temperature and plume characteristics.

Hale et al. successfully applied Laser Doppler Velocimetry (LDV) and In-Flight Particle Pyrometry (IPP) to measure particle velocities and temperatures by spraying aluminum wires in a twin arc electric spraying process (Ref 12). They identified higher particle velocities in the central region compared to the outer region of the spray jet. Furthermore, they observed that the particles generated at the anode connected wire are larger and thus moved at

S. Zimmermann, M. Kauffeldt, K. Landes, and **J. Schein**, Institute of Plasma Technology and Mathematics, Universität der Bundeswehr München, Neubiberg, Germany; and **E. Vogli, M. Abdulgader, B. Krebs, B. Rüther,** and **W. Tillmann**, Institute of Materials Engineering, Technische Universität Dortmund, Dortmund, Germany. Contact e-mails: jochen.schein@UniBw.de and wolfgang.tillmann@udo.edu.

lower velocities than the particles generated at the cathode. The same effect had been determined by variation of the atomization gas stream. The lower the gas flow rate, the larger the particles and lower the particle velocities are. The same conclusion was drawn by Pormousa et al. (Ref 10) and Planche et al. (Ref 13) using a DPV 2000 system during twin arc spraying of carbon steel and stainless steel wires, respectively, as well as by Tillmann et al. employing an Accuraspray-g3 system (Ref 14-16). The experiments and diagnostic measurements by means of DPV2000 showed no significant influence of wire feed rate and operating arc voltage on particle size (Ref 10).

The evaluation of particle velocity and temperature during twin wire arc spraying was also carried out using cored wires by means of Accuraspray-g3 (Ref 14-16). Independent of the kind of wires used the highest particle acceleration took place from the point of arc ignition up to a 50 mm stand-off distance, while at stand-off distances between 100 and 150 mm the velocity reached its highest value. An area of particle deceleration followed at stand-off distances larger than 150 mm. It was observed that the particle velocities generated by spraying of cored wires were about 30% less than that of massive wires, whereas the particle temperatures of massive wires were larger than the particle temperatures of the cored wires. Particle properties are also strongly dependent on nozzle design (Ref 17-19). LDA investigations on arc spraying of Co-based cored wires demonstrated an increase of particle velocities of approximately 20% by using a laval-type nozzle compared to a commonly used straight nozzle (Ref 18). These measured values were verified by CFD calculations. Bach et al. applied CCD camera and Particle Image Velocity (PIV) to diagnose on-line the magnitude and distribution of the particle velocities during arc spraying of X45Cr13 steel wires (Ref 19). A velocity increase of approximately 10% was detected by application of a high-speed cap nozzle in the arc-gun.

Even though diagnostic systems are state-of-the-art in arc spray processes, the accuracy and the comparability of different systems for this process is up to now unclear. The aim of this study was to understand the particle behavior during arc spraying with cored wires at different process parameters and to evaluate two different diagnostic systems: LDA and Accuraspray-g3.

2. Experimental Conditions

2.1 Wire Feedstock

Fe-cored wires with a 1.6 mm diameter (AS 850, Co., Durum, Germany) were employed as feedstock material. They consist of a Fe-velum filled with irregular and broken hard particle powders with a size between 38 and 150 μm. Filling coefficient of cored wire is 52 wt.% and their composition 2% C, 4% Cr, <1% Mn, 1.4% Si, 50% fused WC and Fe Bal. Figure 1 illustrates the cross-section of the used metal-cored wires as well as the filling powders morphology analyzed by light and scanning electron microscopy.

2.2 Coating Process

To study the on-line particle characteristics during arc spraying by means of cored wires and to evaluate two different diagnostic systems, a twin wire arc spraying facility (Smart Arc PPT 350, Sulzer Metco, Switzerland) was used. This system operates through a current-controlled modus, where the current intensity is coupled with wire feeder velocity. By applying current at the contact point of the consumable cored wires, which are connected as cathode and anode, a short circuit is generated and the cored wires tips are melted. The melted wires are atomized and accelerated through the primary gas stream (so-called primary atomization gas). To focus the spray jet a secondary gas stream is used (so-called secondary gas).

In this research work, two different air cap inserts—commercial air cap insert (Sulzer Metco, Switzerland, Fig. 2a) using only primary atomization gas and commercial fan-shaped air cap insert using primary and secondary gas with four micro-jet-channels asymmetrically surrounding the central bore (Sulzer Metco, Switzerland, Fig. 2b)—were employed to study the influence of secondary gas pressure on the particle formation and properties. Compressed air was used as both primary and secondary gas stream.

To study the influence of the secondary gas stream on particle properties in-flight, the primary atomization gas pressure was kept constant with 0.6 MPa, while the secondary gas pressure was varied between 0 and 0.4 MPa.

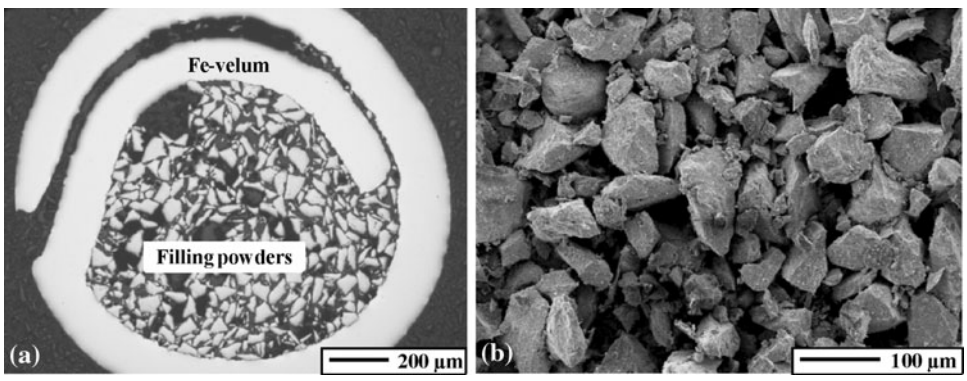

Fig. 1 (a) Cross-section of used Fe-cored wires taken by light microscopy and (b) filling powder taken by scanning electron microscopy

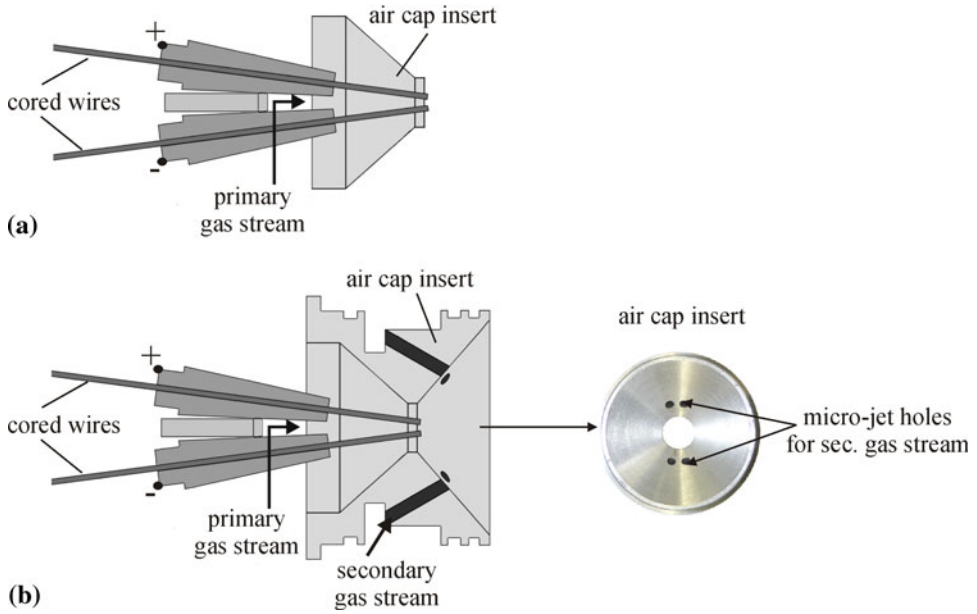

Fig. 2 Schematic diagram of used arc spraying device (a) without and (b) with secondary gas stream

Table 1 Applied parameters

Setup no.	Primary atomization gas pressure, MPa	Secondary gas pressure, MPa	Current, A	Voltage, V
1	0.6	0.2	280	28
2	0.6	0.4	280	28
3	0.6	0.2	180	30
4	0.6	0.4	180	30
5	0.6	0	180	30
6	0.6	0	280	30

Using ''one-factor-at-a-time'' variation the influence of voltage as well as the current on in-flight particles characteristics was also studied (Table 1). The measurements with both diagnostic systems were performed at stand-off distances of 45, 60, 90, 125 and 160 mm to analyze particle behavior during flight.

2.3 In-Flight Particle Diagnostics

To investigate the in-flight particle properties such as temperature and velocity, the Accuraspray-g3 device was employed (Tecnar, Canada, Fig. 3). This device consists of a controller and a sensor head. During the experiments described here the measurements were carried out using a sensor head type H, fitted for high-temperature processes such as arc spraying. The temperature and velocity of in-flight particles were defined as a mean value of all particles within two measurement volumes with a dimension of 3 mm in diameter and 25 mm in length. The measurement volumes result from the optical projection of two circular openings in the optics of the Accuraspray-g3 measuring head. Furthermore, the volume depth is given from field-of-depth of the projection around the focus. If particles pass through the measurement volume, their emitted light

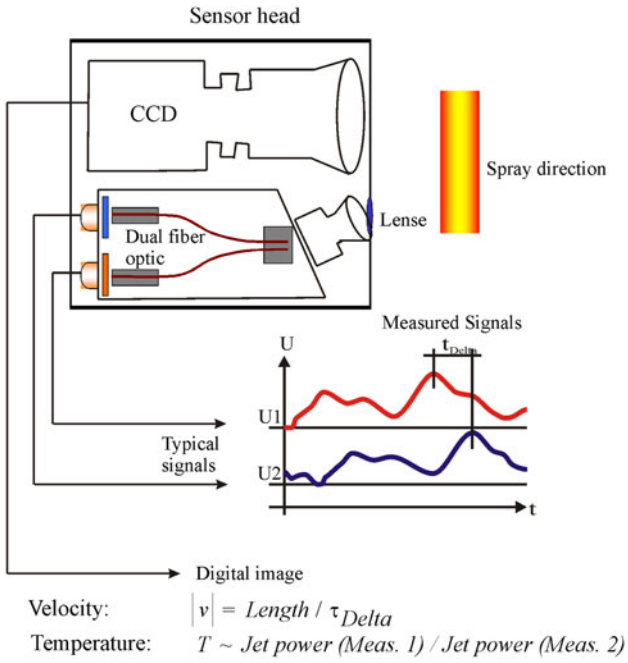

Fig. 3 Accuraspray-g3 principle

is received by the optics through the circular openings. The incoming radiation is afterwards converted using a pin diode into a voltage, which is then evaluated.

Through a dual fibre optical system the flow of particles is detected at two different points along the spray jet. The velocity is determined as a ratio of the distance between the two measuring points and the time delay. Mean particle temperature is defined based on the dual wavelength

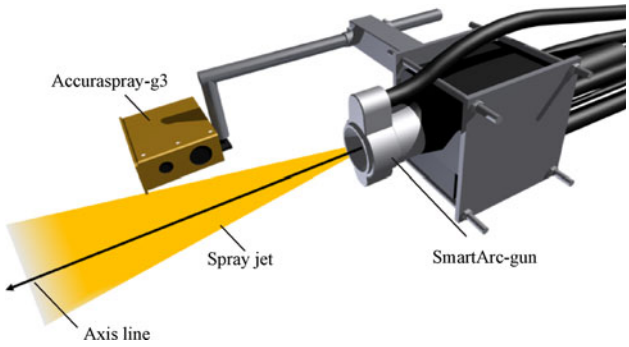

Fig. 4 Self-constructed device to fix Accuraspray-g3 head

pyrometer principle, assuming the emissivity of the particles to be the same for both wavelengths. A correlation threshold between 0 and 1 ensures that both pyrometers detect the same particle density. In our measurements the correlation threshold was 0.6.

The measuring device was located at different stand-off distances along the spray jet axis for all setups using a self-constructed device (Fig. 4). The device was installed on the spray gun to ensure a constant distance of 200 mm between sensor head and the center of the spray jet and to conveniently adjust the stand-off distances along the spray jet. Particle velocity and temperature were recorded for every experimental setup. The data obtained were analyzed and evaluated with respect to the process parameters.

2.4 Setup and Function of the Particle Diagnostic System LDA (Laser-Doppler-Anemometry)

The diagnostic system LDA is a flexible and well-established method to investigate, none intrusively, the local velocity components of gases, liquids or multicomponent flow mixtures with the help of tracer particles. Available LDA configurations are being produced by DantecDynamics and TSI (Ref 20, 21) and interesting setups (Ref 22-32) and developments (e.g., mobile robust system miniaturization) (Ref 28) are accomplished. The LDA system is a light scattering method to determine the velocity of the scattering centers. The classification of the light scattering process is carried out according to the Mie parameter q which describes the ratio between the size and the incident wavelength. Scattering is thus divided into $q \ll 1$ Rayleigh scattering, $q \approx 1$ Mie scattering (the typical range for LDA), $q \gg 1$ geometric optics. The Mie parameter q is defined as:

$$q = \frac{\pi d_p}{\lambda_{laser}}$$

with d_p the particle diameter and λ_{laser} the wavelength of the laser beam. Figure 5 represents the dependence between the intensity of the scattered light and the diameter of the scattering center, the latter assumed to be spherical.

The LDA process can be explained in two alternative but equivalent ways (Ref 27-32): as interference pattern and by means of the Doppler effect. In the first explanation,

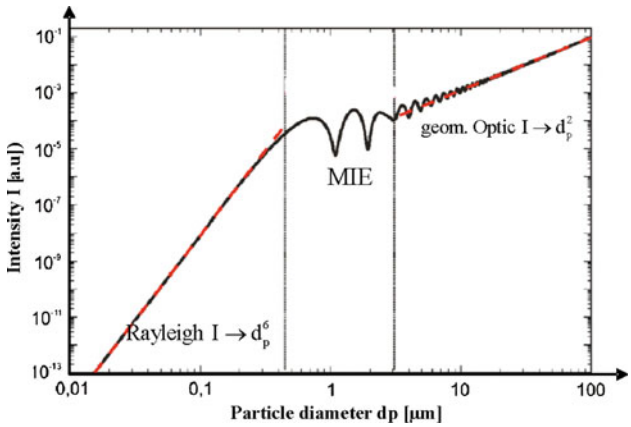

Fig. 5 Scattered intensity as a function of the diameter of a spherical scattering center

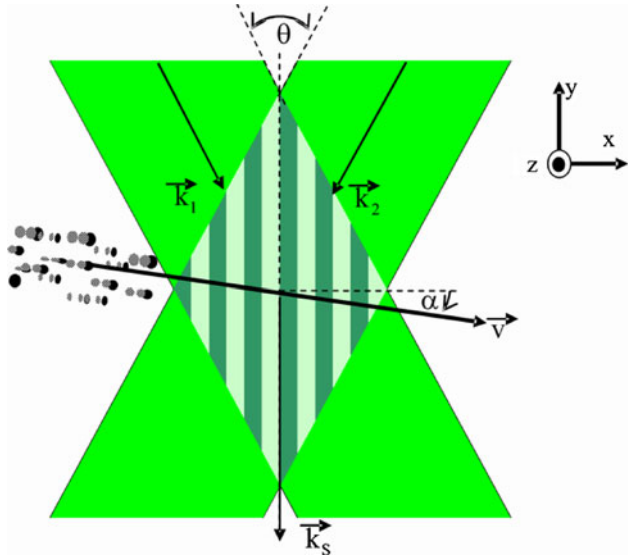

Fig. 6 Measurement volume and LDA explanation according to the interference pattern

two laser beams are superposed in the measurement volume and produce a periodic pattern of intensity maxima and minima parallel to the bisecting line of the beams (Fig. 6).

The distance d between two consecutive maximum and minimum and the velocity component v_x perpendicular to the interference fringes are calculated according to

$$d = \frac{\lambda_{laser}}{2\sin(\theta/2)}$$

$$v_x = v\cos\alpha = df$$

with θ the angle between the two incident laser beams, α the angle between the flow direction and the interference fringes and f the frequency of the measured scattering signal. Those particles flying across the measurement volume produce a periodic scattering signal when crossing

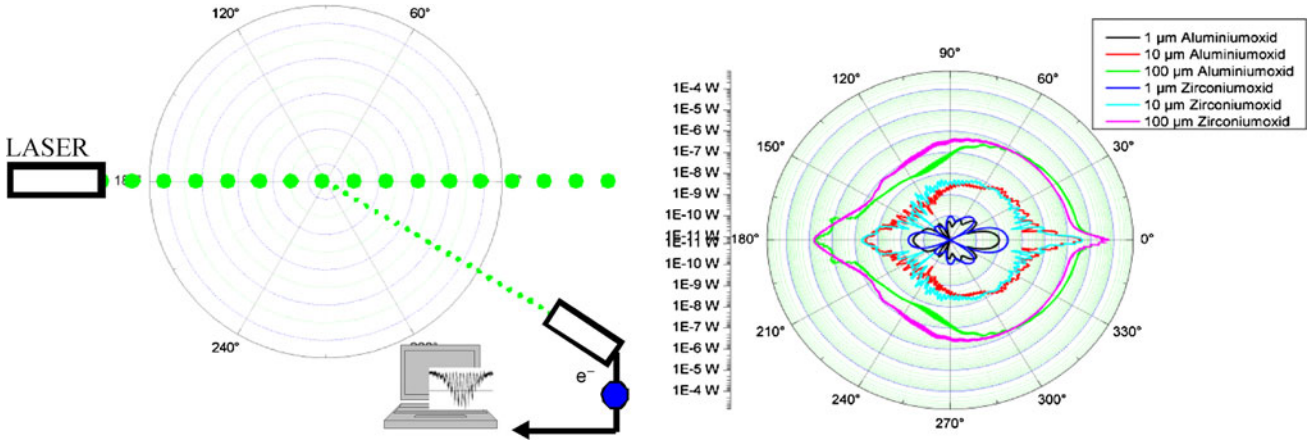

Fig. 7 Detection of the angle dependence and scattering intensity as a function of particle size (for ceramic powders of Al_2O_3 and ZrO_2)

the interference fringes. A photomultiplier records these signals from different angle directions. The intensity of the signal depends on the detection angular direction and the object size (particle diameter). Assuming spherical particles and using the Mie theory (Ref 29), this angular function can be determined (Fig. 7). Alternatively, the slight Doppler shift in the light scattered by the flying particles can be applied. The Doppler effect is described by the two wave vectors $\vec{k}_1$ and $\vec{k}_2$ of the incident laser beams and by the resulting scattering wave vector $\vec{k}_S$ (Fig. 6). The velocity of the scattering centers is correlated to the difference in the frequency Δf for the Doppler shift between the scattered signals from the two beams

$$\left|\vec{k}_1 - \vec{k}_2\right| = 2\left|\vec{k}_1\right| \sin\left(\frac{\theta}{2}\right) = \frac{4\pi}{\lambda_{\text{laser}}} \sin\left(\frac{\theta}{2}\right)$$

$$\Delta f_{\text{beam1}} = \frac{\left(\vec{k}_1 - \vec{k}_S\right) \cdot \vec{v}}{2\pi}, \; \Delta f_{\text{beam2}} = \frac{\left(\vec{k}_2 - \vec{k}_S\right) \cdot \vec{v}}{2\pi}$$

$$\Delta f_D = \Delta f_{\text{beam1}} - \Delta f_{\text{beam2}} = \frac{\left(\vec{k}_1 - \vec{k}_2\right) \cdot \vec{v}}{2\pi} = \frac{2v \cos\alpha}{\lambda_{\text{laser}}} \sin\left(\frac{\theta}{2}\right)$$

where Δf_D is the measured difference in the frequency of the Doppler shift.

2.5 Investigations of Particle Behavior During the Wire Arc Spray Process by the LDA System

The principle of the applied and used LDA-Forward-Scattering technique is depicted in Fig. 8(a) and the experimental setup is shown in Fig. 8(b). The LDA permits precise determination of local particle density and velocity, as thermal emission of spray particles is not necessary and also does not influence the measured values.

The beam of a cw-laser is splitted by transmitting optics in two beams of equal intensities. Their crossing zone is the measuring volume. A particle moving in this volume is illuminated by the two laser beams. Consequently, it scatters light at two Doppler shifted frequencies. In the photomultiplier, the recorded radiation is transformed into an electrical signal called ''laser burst'' used for the determination of the particle velocity v_x. With the velocity and signal rate, additional relevant properties of the particle flux like trajectories, dwell times and isotaches can be determined. The measurement grid and the distance between Smart Arc and first measurement plane (x-plane) are depicted in Fig. 9. Note that the particle size cannot be measured by the LDA method because there is no unequivocal relation between the particle size and the laser burst signal.

3. Results and Discussion

Depending on the process parameters and the kind of the employed air cap insert, different spray jet characteristics were detected. By employing secondary gas and fan-shaped air cap insert, the spray jet shape was modified from a dispersed and wide spray jet to a more focused and dense one (Fig. 10). The primary gas atomizes the melted metal on the wire tips, while the secondary gas stream concentrates the flow pattern of the spray jet through a conical sheath around the axial spray jet. A jet width reduction of ~10% measured by means of Accuraspray-g3 was identified. This confirms that applying of a fan-shaped air cap insert within a closed nozzle system is associated with less plume divergence. To the same conclusion came Gedzevicius et al. (Ref 17) and Wang et al. (Ref 33) by spraying of metallic wires via arc spraying. Spray jet shape changing has also a strong influence on the in-flight properties of generated particles.

3.1 Accuraspray-g3 Results

The measured values of velocity and temperature at different stand-off distances are illustrated in Fig. 11-13. It is obvious that at a stand-off distance of ~60 mm the particle velocity becomes smaller and increases again at larger stand-off distances for all setups when employing a secondary gas stream. In contrast to these measurements,

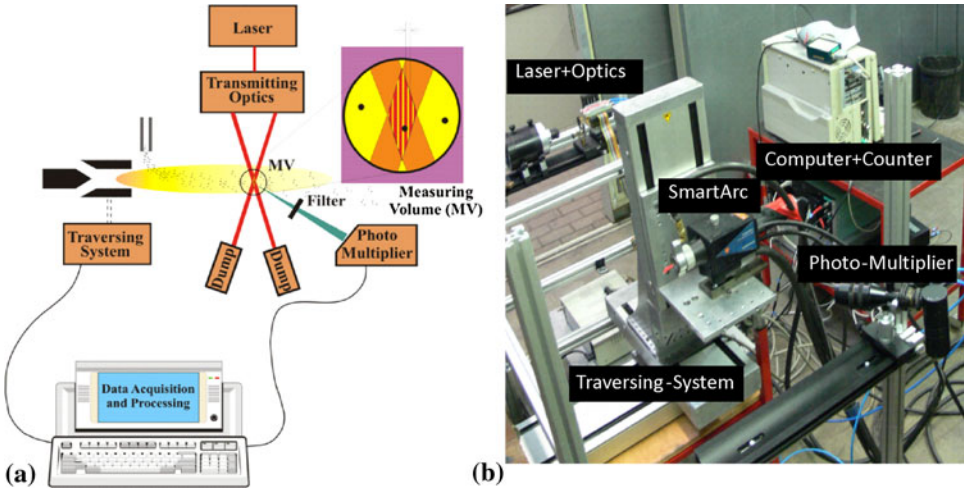

Fig. 8 (a) Principle of the used LDA-Forward-Scattering technique (Laser: Compass 315M laser Coherent, Nd-YAG Laser 100mW; Photodetector: Dantec 57X08PM (500 MHz) Data Acquisition: Dantec Counter Processor 55L90a; Computer + ASYST-Software) and (b) experimental setup

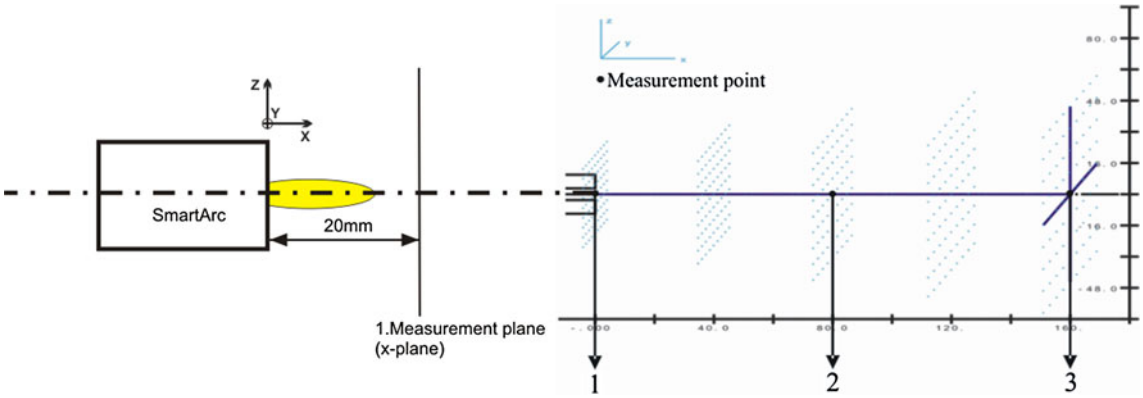

Fig. 9 Measurement distance between Smart Arc and first plane (investigation offset 20 mm); measurement grid with 5 × 9 × 9 points

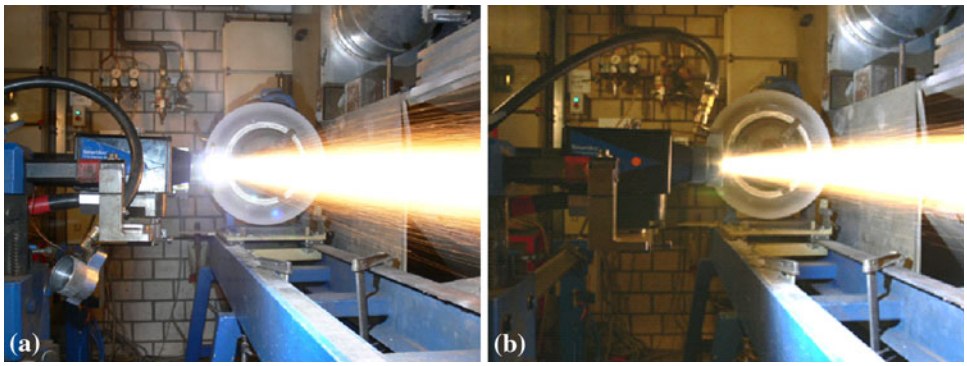

Fig. 10 Spray jet by using (a) standard air cap insert without secondary gas and (b) fan-shaped air cap insert

only an increase of velocity with stand-off distance can be observed for the particles in spray jets produced for setups 5 and 6 without secondary gas. This different behavior was explained by Tillman et al. (Ref 15) and verified by means of CFD-modeling through the large turbulences in this area.

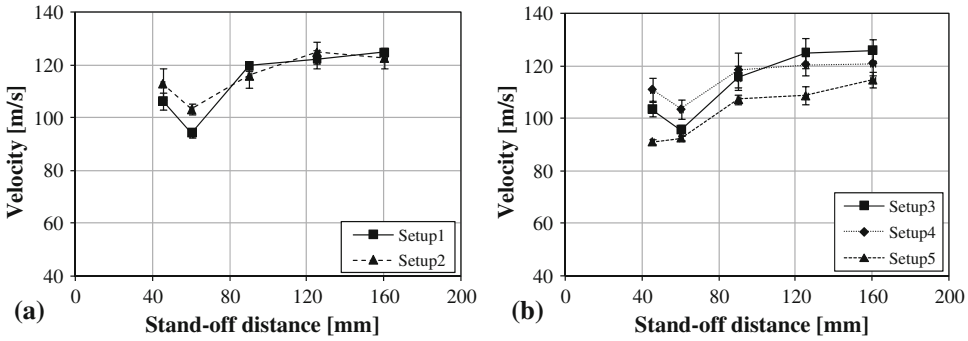

Fig. 11 (a, b) Variation of particle velocities at different setups

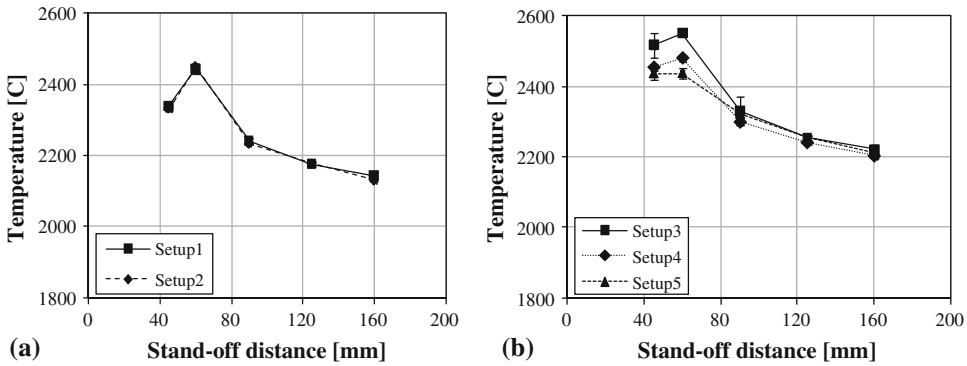

Fig. 12 (a, b) Variation of particle temperatures at different setups

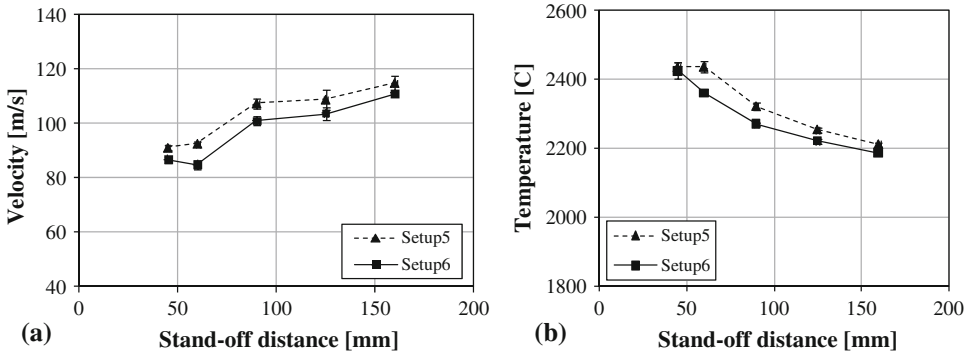

Fig. 13 Variation of (a) particle velocity and (b) particle temperatures at setups without secondary gas stream

In this area a crossing of two streams occurs. The primary atomization air stream flows axially, while the secondary gas stream is orientated 45° to the axial stream. Furthermore, both streams possess different temperatures. The primary air stream is heated through the atomization of the melted wire bath, while the secondary gas stream has the environment temperature. Cold secondary gas stream admittance into a warm high-speed primary stream rapidly increases the fluctuations in the axial directions due to swirling eddies and entrainment of external air. Thus at this area a strong deceleration of particles is observed. The particles are blocked, collide with each other and thereby the velocity is decreased. To the same conclusion came Spores et al. (Ref 34) by studying a turbulent thermal plasma jet in the case of atmospheric plasma spraying. This phenomenon was also verified in setups without secondary gas stream in this research work. The results of setup 5 and 6 show a continual increase of particle velocity with stand-off distance (Fig. 11b and 13a). Regardless of the system parameters setup, larger particle velocities are attained with the use of primary and secondary gas streams compared with the use of primary gas stream only (Fig. 11b). This can be explained through the higher air flows and thereby higher net drag force

vector by employment of the secondary gas stream compared to the experiments without secondary gas.

Exactly in the turbulences area a slight increase of particle temperature was identified for all setups carried out with the fan-shaped air cap insert using primary and secondary gas. Ervine et al. (Ref 35) and Wu et al. (Ref 36) examined a particle break-up in the high-speed jet through turbulences in the gas phase. They identified turbulences as the primary initiator of droplets break-up. Hussary et al. (Ref 37) named this process ''secondary atomization'' by studying arc spraying with metallic wires. To the same conclusion came Tillmann et al. (Ref 15) by studying cored wire arc spraying by means of high-speed camera. Thereby smaller particles could be generated in this area, resulting in an increase in the surface to volume of the particles. Two phenomena take place in this zone. Firstly, the air-Fe exothermic reaction enhances due to the increasing surface to volume of the particles. Secondly, using secondary gas stream indicates an enhanced convective cooling of the particles. Since for the setups 1 to 4 the particle temperatures increase at 60 mm indicate that the first phenomenon dominates. With increasing secondary gas stream the cooling effect increases and in setup 6 a reducing particle temperature was detected. With increasing stand-off distance the particles cooled down through contact with cool environment air for all setups (Fig. 12 and 13b). The variation of voltage or current does not show any significant influence on the particle properties for all setups with secondary gas stream.

Completely different particle behaviors were observed in case of setups without secondary gas (setup 5 and 6, Fig. 13). The particles in the setup 6 show both lower velocities and temperatures at all stand-off distances than the particles from setup 5. The arc power in setup 5 (5.4 kW) is lower compared to the power in setup 6 (8.4 kW). For this reason, the amount of totally melted wires was higher in case of setup 6 than in setup 5. Under the same atomization gas flow, the higher amount of melted bath in setup 6 was atomized into larger particles than in setup 5. Larger and heavier particles move under the same flow conditions slower than the finer particles. Furthermore, they lost, due their low velocity, more thermal energy than the faster moving particles. To the same conclusions came Hussary et al. (Ref 37) by studying of metallic arc spraying process.

3.2 LDA Results

With a *xyz* traversing system the single measurement point can be started and investigated. This additional tool enables measurement of volume from the complete arc wire spray process. The measurement time depends on the count of points per plane (see Fig. 9).

In Fig. 14 the velocity distribution of points 1, 2, and 3 (in axis line of Smart Arc and center of plane) for setup 6 are shown. The results show a particle velocity increase by increasing stand-off distance. This is in agreement with the results of Accuraspray-g3 (Fig. 13a). With all points of the LDA, different contour or surface plots of the density and

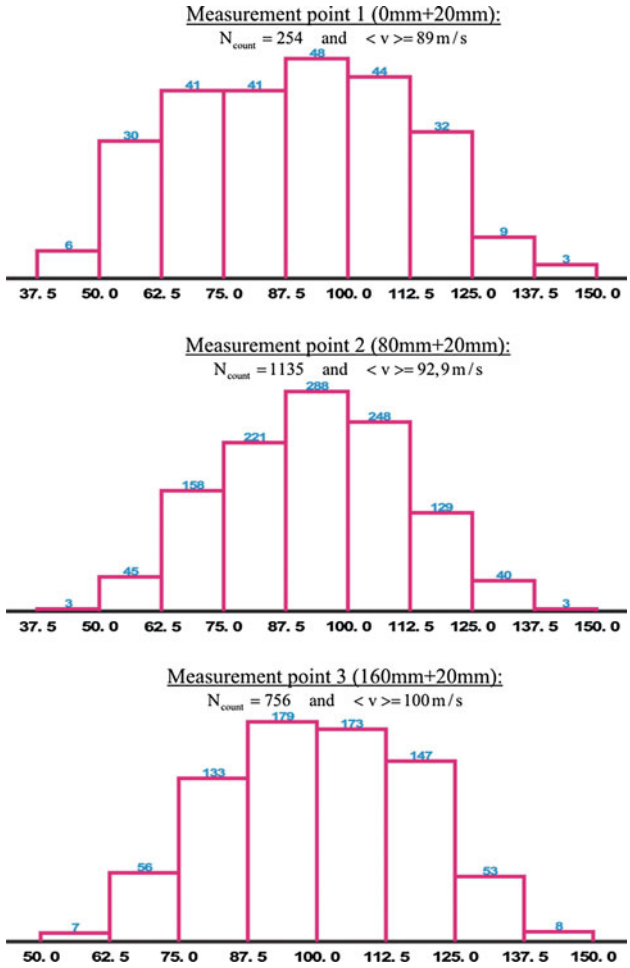

Fig. 14 Velocity distribution at special points 1, 2, and 3 in axis line of Smart Arc for setup 6 ($I = 280$ A, $U = 30$ V, primary pressure 0.6 MPa)

velocity can be calculated and presented (Ref 18, 38-40) (Fig. 15).

It is obvious that the arc spray jet is not homogenous near the arc ignition (Fig. 15a, stand-off 20 mm). It confirms the assumption that the particles generated in negative connected wire possess larger velocities than the particles generated in positive connected wire. In-flight, this difference decreases due to turbulence, and particle velocity profile becomes more homogenous in comparison to the arc ignition area (Fig. 15b). However, in all cases, the particles in the spray jet center fly with higher velocities than the particles in the spray jet outer regions.

Contour plots and particle densities in axis line for setups 4 and 5 are shown in Fig. 16. LDA measurements reveal the same plume behavior as defined by Accuraspray-g3 results. The plumes possess the same width for both setups up to a stand-off distance of 60 mm. With increase of stand-off distance a plume width reduction was observed for setup 4, where a secondary gas stream was used. Exactly in this area turbulences occur and a plume

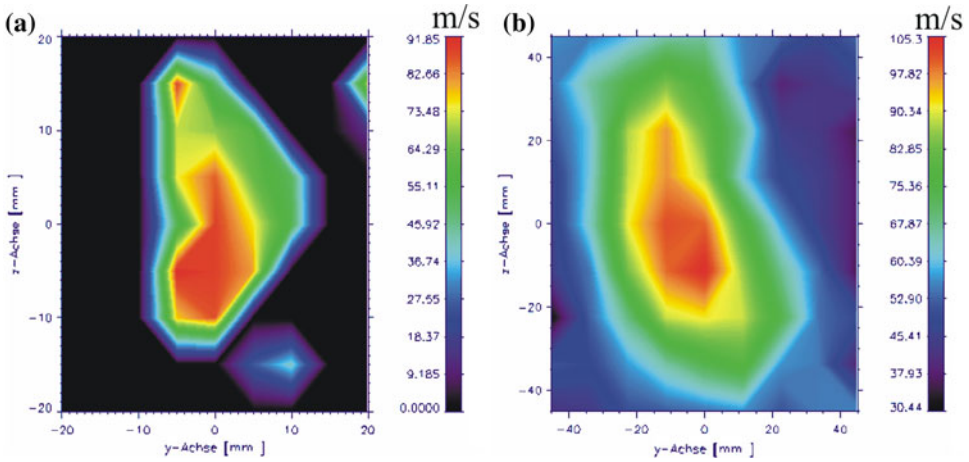

Fig. 15 Contour plot (x-plane) of velocity distribution at position (a) 20 mm and (b) 180 mm behind Smart Arc exit for setup 6 ($I = 280$ A, $U = 30$ V, primary pressure 0.6 MPa)

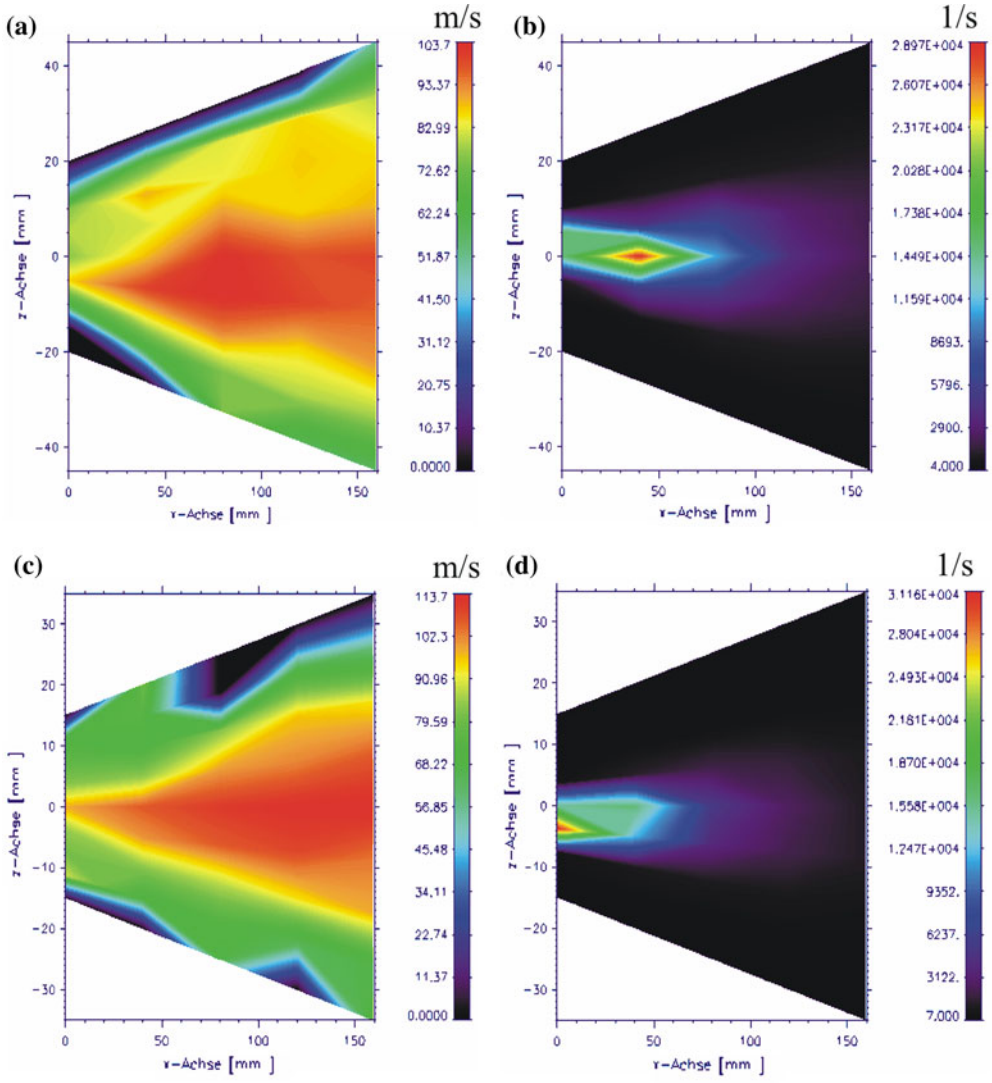

Fig. 16 Contour plot (y-plane) of velocity and number density distribution in axis line of (a, b) setup 4 ($I = 180$ A, $U = 30$ V, primary pressure 0.6 MPa, secondary pressure 0.4 MPa); (c, d) setup 5 ($I = 180$ A, $U = 30$ V, primary pressure 0.6 MPa), respectively

Table 2 Comparison of velocity results at different stand-off distances investigated by Accuraspray-g3 and LDA

Setup no.	Accuraspray-g3, m/s	LDA, m/s	Offset $f_1 = \frac{v_{Accuraspray-g3}}{v_{LDA}}$	Offset $f_2 = \frac{v_{LDA}}{v_{Accuraspray-g3}}$
Stand-off distance 60 mm				
1	98	78	1.256	0.796
2	102	92	1.109	0.902
3	98	108	0.907	1.102
4	102	108	0.944	1.059
5	96	98	0.980	1.021
6	84	88	0.955	1.048
Stand-off distance 120 mm				
1	122	90	1.356	0.738
2	124	90	1.378	0.726
3	122	112	1.089	0.918
4	120	118	1.017	0.983
5	108	102	1.059	0.944
6	102	105	0.971	1.029

focusing take place. Furthermore, the plume width is reduced from 80 mm in setup 5 to 60 mm in setup 4 at a stand-off distance of 150 mm. These phenomena are in agreement with Accuraspray-g3 observations.

In comparison of the particle velocity determination during the wire arc process, the factors $f_1 = \frac{v_{Accuraspray-g3}}{v_{LDA}}$ and $f_2 = \frac{v_{LDA}}{v_{Accuraspray-g3}}$ indicate the offset between Accuraspray-g3 and LDA at different points (Table 2). Even though the used diagnostic systems work under different measurement principles, the results obtained show small differences. Two special contour plots (y-plane) are depicted in Fig. 16 where the factors f_1 and f_2 are near 1, which means an unambiguous conformity of velocity investigation. This fact is a powerful help for controlling and monitoring the wire arc process and can be used to increase the level of reliability and consistency.

4. Conclusion and Outlook

In this study, the influences of different SmartArc configurations and parameters are investigated for the kinetic behavior and interactions of the particles with environment during flight. The Accuraspray-g3 measured the particle velocity and temperature and the LDA determined the particle velocity and number density. The combination of Accuraspray-g3 and LDA allows, in a non-intrusive and online procedure, a reliable and partially redundant determination, a set of the relevant particle velocity parameters. In this first study, the conformity of the velocity distribution for different wire arc setup parameters can be calculated and carried out by using both diagnostic systems. Future measurement with different wire materials, different gases and nozzles will offer the possibility to compare the two different diagnostic systems and to define more characteristic describing factors for the reliability and consistency in the arc spray process.

Acknowledgments

The authors gratefully acknowledge the financial support of the DFG (German Science Foundation) and AiF (German Working Group of Industrial Research Association) within the Collaborative Research Center SFB 708 and within Research Center ''Thermal Spraying''.

References

1. M. Nakagawa, K. Shimoda, T. Tomoda, M. Koyama, Y. Ishikawa, and T. Nakajima, Development of Mass Production Technology of Arc Spraying for Automotive Engine Aluminum Alloy Valve Lifters, *Thermal Spray Research and Applications*, T.F. Bernecki, Ed., May 20-25, 1990 (Long Beach, CA), ASM International, 1991, p 457-464
2. K. Nassenstein, ''Herstellen von partikelverstärkten Metallmatrix-Verbundwerkstoffen durch kombiniertes Lichtbogen- und Hochgeschwindigkeitsflammspritzen (Manufacturing of Particle Reinforced Metal-Matrix Composites Through Arc and High Velocity Oxygen Fuel Spraying),'' Ph.D. Thesis, Dortmund University, 1997 (in German)
3. H.-D. Steffens, M. Dvorak, and M. Wewel, Einfluss der Prozessparameter beim Lichtbogenspritzen - Ein Leitfaden für den Praktiker (Influence of Process Parameters on Arc Spraying—A Guideline for Practitioner), Thermische Spritzkonferenz, Aug 29-31, 1990 (Düsseldorf, Germany), DVS Deutscher Verband für Schweißen, 1990, p 23-26 (in German)
4. A.J. Allen, G.G. Long, H. Boukari, J. Ilavsky, A. Kulkarni, S. Sampath, H. Herman, and A.N. Goland, Microstructural Characterization Studies to Relate the Properties of Thermal Spray Coatings to Feedstock and Spray Conditions, *Surf. Coat. Technnol.*, 2001, **146-147**, p 544-552
5. Y. Yeh and H.Z. Cummins, Localized Fluid Flow Measurements with a He-Ne-Spectrometer, *Appl. Phys. Lett*, 1964, **4**(10), p 176-178
6. J. Agapagis and T. Hoffmann, Real-Time Imaging for Thermal Spray Process Development and Control, *J. Therm. Spray Technol.*, 1992, **1**(1), p 19-25
7. M.F. Smith, Laser Measurements of Particle Velocities in Vacuum Plasma Jets, *Tagungsband of 1st Plasma Technik Symposium*, Vol 1, H. Eschnauer, Ed., May 18-20 (Lucerne, Switzerland), 1988
8. T.V. Streibl, T. Duda, and K.D. Landes, Diagnostics of Thermal Spray Processes by In-Flight Measurement of Particle Size and Shape with Innovative Particle-Shape-Imaging (PSI) Technique, *SPIE, High Speed Imaging and Analysis III*, Vol 4308, A.M. Frank, Ed., Jan 21-26 (CA), 2001, p 45-52
9. N. Hussary, J. Schein, J. Heberlein, Control of Jet Convergence in Wire Arc Spray Systems, Tagungsband Conference Proceedings, E. Lugscheider and R. A. Kammer, Ed., March 17-19 (Düsseldorf, Germany), 1999, p 335-339
10. A. Pourmousa, J. Mostaghimi, A. Abedini, and S. Chandra, Particle Size Distribution in a Wire-Arc Spraying System, *J. Therm. Spray Technol.*, 2005, **14**(4), p 502-510
11. J. Stanisic, D. Kosikowski, and P.S. Mohanty, High-Speed Visualization and Plume Characterization of the Hybrid Spray Process, *J. Therm. Spray Technnol.*, 2006, **15**(4), p 750-758
12. D.L. Hale, W.D. Swank, and D.C. Haggard, In-Flight Particle Measurements of Twin Wire Electric Arc Sprayed Aluminum, *J. Therm. Spray Technol.*, 1998, **7**(1), p 58-63
13. M.P. Planche, H. Liao, and C. Coddet, Relationships Between In-Flight Particle Characteristics and Coating Microstructure with a Twin Wire Arc Spray Process and Different Working Conditions, *Surf. Coat. Technol.*, 2004, **182**, p 215-226
14. W. Tillmann, E. Vogli, and M. Abdulgader, Diagnostics of Cored Wire Arc Spraying for Wear Resistant Coatings, *The Coating in Manufacturing Engineering*, Vol 10, Fr.-W. Bach, K.D. Bouzakis, B. Denkena, and M. Geiger, Ed., Oct 25-26 (Hannover, Germany), 2007, p 323-332

15. W. Tillmann, E. Vogli, M. Abdulgader, S. Turek, and M. Gurris, Particle Formation During Arc Spraying with Cored Wires, *J. Therm. Spray Technol.*, 2008, **17**(5-6), p 966-973
16. W. Tillmann, E. Vogli, and M. Abdulgader, Asymmetric Melting Behavior in Twin Wire Arc Spraying with Cored Wires, *J. Therm. Spray Technol.*, 2008, **17**(5-6), p 974-982
17. I. Gedzevicius, R. Bolot, H. Liao, C. Coddet, and A.V. Valiulis, Application of CFD for Wire-Arc Nozzle Geometry Improvement, *Thermal Spray 2003: Advancing the Science and Applying the Technology*, B.R. Marple and C. Moreau, Ed., May 5-8, 2003 (Orlando, FL), ASM International, 2003, p 977-980
18. J. Wilden, J.P. Bergmann, A. Schwenk, K. Landes, and S. Zimmermann, Supersonic Nozzles for the Wire Arc Spraying, *International Thermal Spray Conference*, E. Lugscheider and C.C. Berndt, Ed., Mar 4-6, 2005 (Basel, Switzerland), DVS Deutscher Verband für Schweißen, 2005, p 1068-1073
19. Fr.-W. Bach, D.T. Copitzky, G. Tegeder, and J. Prehm, Einsatz der PIV-Technik zum Bestimmen des Einflusses unterschiedlicher Düsengeometrien auf den Lichtbogenspritzprozess (Application of PIV-Technique to Determine the Influence of Different Nozzle Geometries on the Arc Spraying Process), *International Thermal Spray Conference*, E. Lugscheider and C.C. Berndt, Ed., Mar 4-6 (Essen, Germany), DVS Deutscher Verband für Schweißen, 2002, p 450-453 (in German)
20. www.DantecDynamics.com
21. www.TSI.com
22. G. Gouesbet, A Review on Measurements of Particle Velocities and Diameters by Laser Techniques, with Emphasis on Thermal Plasmas, *Plasma Chem. Plasma Process.*, 1985, **5**(2), p 91-117
23. P. Fauchais, J.F. Coudert, and M. Vardelle, Diagnostics in Thermal Plasma Processing, *Plasma Diagnostics*, 1989, p 410-432
24. H.D. vom Stein, H.J. Pfeifer, and B. Koch, Geschwindigkeitsmessungen an kurzzeitigen Strömungsvorgängen mittels Laserstrahlung (Velocity Measurements on Short-Time Flow Phenomena through Laser Radiation), *Opt. Commun.*, 1969, **1**, p 207-210 (in German)
25. H.J. Pfeifer and H.D. vom Stein, A Measuring Technique to Determine the Turbulence Degree in Gas Flows with a CW-laser, *Opt. Commun.*, 1971, **3**, p 387-390
26. S. Hanson, Broadening of the Measured Frequency Spectrum in a Differential Laser Anemometer due to Interference Plane Gradients, *J. Phys. D: Appl. Phys.*, 1973, **2**, p 164-172
27. F. Durst, A. Melling, and J.H. Whitelaw, *Principles and Practices of Laser-Doppler Anemometry*, Academic Press, London, 1976, p 412
28. M. Hugenschmidt, Lasermesstechnik, Diagnostik der Kurzzeitphysik (Laser Measuring, Diagnostics of Short-Time Physics), Springer, 2007, p 131-142
29. G. Mie, Beiträge zur Optik trüber Medien, spezielle kolloidale Metallösungen (Contribution to Optics Cluded Media, Special Colloidal Metal Solutions), *Ann. Phys. Berlin*, 1908, **330**, p 377-445
30. W. Mayr, "Bestimmung der lokalen Geschwindigkeits- und Größenverteilung von Partikeln im Plasmastrahl mittels Laser-Doppler-Anemometrie (Determination of Local Velocity and Size Distribution of Particles in Plasma Jet Through Laser-Doppler-Anemometry)," Ph.D. Thesis, UniBw München, 1983 (in German)
31. F. Durst, A. Melling, and J. Whitelaw, Theorie und Praxis der Laser-Doppler-Anemometrie (Theory and Practice of Laser-Doppler-Anemometry), G. Braun-Verlag Karlsruhe, 1987
32. A. Reusch, "Die Entwicklung eines Laser-Doppler-Meßsystems und seine Anwendung bei Verfahren des thermischen Beschichtens (Development of a Laser-Doppler-Measuring System und its Application for Thernal Spraying)," Ph.D. Thesis, UniBw München, 1995 (in German)
33. X. Wang, J. Heberlein, E. Pfender, and W. Gerberich, Effect of Nozzle Configuration, Gas Pressure and Gas Type on Coating Properties in Wire Arc Spray, *J. Therm. Spray Technol.*, 1999, **8**(4), p 565-575
34. R. Spores and E. Pfender, Flow Structure of a Turbulent Thermal Plasma Jet, *Surf. Coat. Technol.*, 1989, **37**, p 251-270
35. D.A. Ervine and H.T. Falvey, Behavior of Turbulent Water Jets in the Atmosphere and in Plunge Pools, *Proc. Inst. Civil Eng.*, 1987, **83**(2), p 295-314
36. P.K. Wu, R.F. Miranda, and G.M. Faeth, Effects of Initial Flow Conditions on Primary Breakup of Nonturbulent and Turbulent Round Jets, *Atomization Spray*, 1995, **5**, p 175-196
37. N. Hussary and J. Heberlein, Metal Droplet Formation Mechanisms in the Wire Arc Spraying Process, *Proceedings of the 48th International Research Colloquium*, Sept 22-25 (Illmenau, Germany), 2003
38. S. Zimmermann and K.D. Landes, LDA and PSI—In Combination a Modern Particle Diagnostic System, 12. Workshop Plasma Technology, TU Ilmenau, Germany, 2004
39. J. Wilden, J.P. Bergmann, S. Jahn, K. Landes, and S. Zimmermann, Influence of the Voltage Modulation Frequency on Voltage Trace and Wire Arc Coatings Properties, *International Thermal Spray Conference*, E. Lugscheider and C.C. Berndt, Ed., Mar 4-6, 2005 (Basel, Switzerland), DVS Deutscher Verband für Schweißen, 2005, p 393-398
40. S. Zimmermann, S. Lange, J.L. Marqués, G. Forster, K. Landes, and J. Schein, Ausgewählte diagnostische Verfahren für den Plasmaspritzprozess (Selected Diagnostic Methods for the Plasma Spray Process), *Therm. Spray Bull.*, 2008, **2**, p 128-138